Nuclear Shadowing and High-p_T Hadron Spectra in Relativistic Heavy Ion Collisions

R. Vogt and S.R. Klein

Nuclear Science Division, Lawrence Berkeley National Laboratory, Berkeley, CA 94720, USA
Physics Department, University of California, Davis, CA 95616, USA

Nuclear Parton Distributions

Nuclear parton densities

$$
\begin{aligned}
F_i^A(x, Q^2, \vec{r}, z) &= \rho_A(s) S^i(A, x, Q^2, \vec{r}, z) f_i^N(x, Q^2) \\
F_j^B(x, Q^2, \vec{b} - \vec{r}, z') &= \rho_B(s') S^j(B, x, Q^2, \vec{b} - \vec{r}, z') f_j^N(x, Q^2)
\end{aligned}
$$

$$
s = \sqrt{r^2 + z^2} \quad \text{and} \quad s' = \sqrt{|\vec{b} - \vec{r}|^2 + z'^2}
$$

$$
\rho_A(s) = \rho_0 \frac{1 + \omega(s/R_A)^2}{1 + \exp[(s - R_A)/d]}
$$

Shadowing functions (Kari Eskola)

$$
\begin{aligned}
S_1 &= S_1(A, x) \ \text{all partons equal, no } Q^2 \text{ evolution} \\
S_2 &= S_2^i(A, x, Q^2) \ q_V,\ q_S, \text{ and } G \text{ evolved over } 2 < Q < 10 \text{ GeV} \\
S_3 &= S_3^i(A, x, Q^2) \ \text{all evolved separately, } 1.5 < Q < 100 \text{ GeV}
\end{aligned}
$$

With no nuclear modifications, $S^i(A, x, Q^2, \vec{r}, z) \equiv 1$.

Spatial dependence of shadowing

Proportional to local nuclear density:

$$
S^i_{\rm WS} = S^i(A, x, Q^2, \vec{r}, z) = 1 + N_{\rm WS}[S^i(A, x, Q^2) - 1] \frac{\rho(s)}{\rho_0}
$$

Proportional to nuclear path length:

$$
S^i_\rho(A, x, Q^2, \vec{r}, z) = 1 + N_\rho (S^i(A, x, Q^2) - 1) \int dz \rho_A(\vec{r}, z) \ .
$$

Normalization: $(1/A) \int d^2r dz \rho_A(s) S^i_{\rm WS,\,R} \equiv S^i$. Larger than average modifications for $b = 0$. Nucleons like free protons when $s \gg R_A$.

Proton Parton Distributions

$Q = 4$ GeV, $q_V = u_V + d_V$, $q_S = \overline{u} + \overline{d} + \overline{s}$

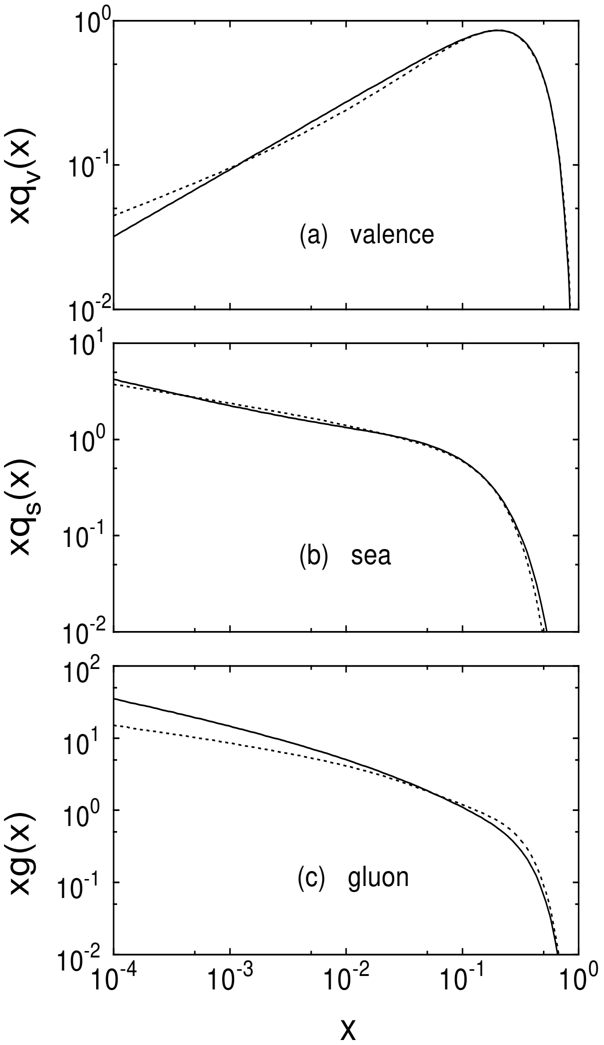

Figure 1: The (a) valence, (b) sea, and (c) gluon distributions in a proton are given at $Q^2 = p_0^2 = 4$ GeV^2 for the GRV 94 LO (solid) and MRST LO (dashed) sets.

Shadowing Parameterizations

- 'Saturation' in ratios at low x for S_1 and S_2
- Gluon evolution strongest
- Sea quark shadowing in S_3 only
- Significant gluon antishadowing in S_3
- Gluon ratio determined by conservation rules, not data

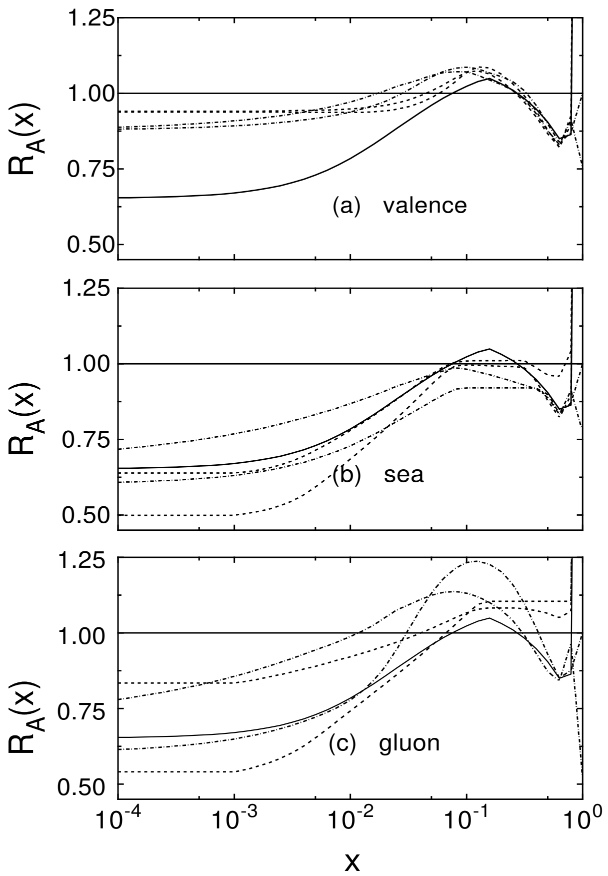

Figure 2: The three shadowing parameterizations for $A = 200$ for (a) valence quarks, (b) sea quarks, and (c) gluons, relative to $S = 1$. The S_1 parameterization is shown in the solid curves. The S_2 ratios are given by the dashed curves. At low x, the lower curves are for $Q = 2$ GeV while the upper are for $Q = 10$ GeV. The S_3 ratios, in the dot-dashed curves, are shown for the u_V and $\overline{u}$. The lower curves at low x are for $Q = 1.5$ GeV while the upper curves at low x are for $Q = 10$ GeV.

Minijet Production

Minijet rapidity distribution at LO

$$
\begin{aligned}
\frac{d\sigma^f(p_0)}{dyd^2bd^2r} &= K_{\rm jet}\int dp_T^2 dy_2 dz dz' \sum_{\substack{ij=\\ \langle kl\rangle}} x_1 F_i^A(x_1,p_T^2,\vec{r},z) x_2 F_j^B(x_2,p_T^2,\vec{b}-\vec{r},z') \\
&\quad \times \left[\delta_{fk}\frac{d\hat{\sigma}}{d\hat{t}}^{ij\to kl}(\hat{t},\hat{u}) + \delta_{fl}\frac{d\hat{\sigma}}{d\hat{t}}^{ij\to kl}(\hat{u},\hat{t})\right]\frac{1}{1+\delta_{kl}}
\end{aligned}
$$

Limits of integration:

$$
\begin{aligned}
p_0^2 &< p_T^2 < S/(4\cosh^2 y) \\
\ln(\sqrt{S}/p_T - e^{-y}) &\leq y_2 \leq \ln(\sqrt{S}/p_T - e^{y}) \\
|y| &\leq \ln(\sqrt{S}/2p_0 + \sqrt{(\sqrt{S}/2p_0)^2 - 1})
\end{aligned}
$$

We take $K_{\rm jet} = 1$, $p_0 = 2$ GeV, $n_f = 4$ and evaluate $\alpha_s(p_T)$ at one-loop. We use MRST LO partons.

Total parton number at impact parameter b:

$$
\begin{aligned}
\overline{N}^f(b,p_0) &= 2\frac{d\sigma^f(p_0)}{d^2b} \\
\overline{N}(b,p_0) &= \sum_f \overline{N}^f(b,p_0)
\end{aligned}
$$

When $S = 1$ or $S = S^i(A,x,Q^2)$, shadowing factorizes and $\overline{N} \propto T_{AB}(b)$ where $T_{AB}(b) = \int d^2r T_A(\vec{r})T_B(\vec{b}-\vec{r})$, $T_A(\vec{r}) = \int dz \rho_A(z,\vec{r})$ and $T_{AA}(0) \approx A^2/(\pi R_A^2) \propto A^{4/3}$.

Minijet Cross Sections, MRST LO

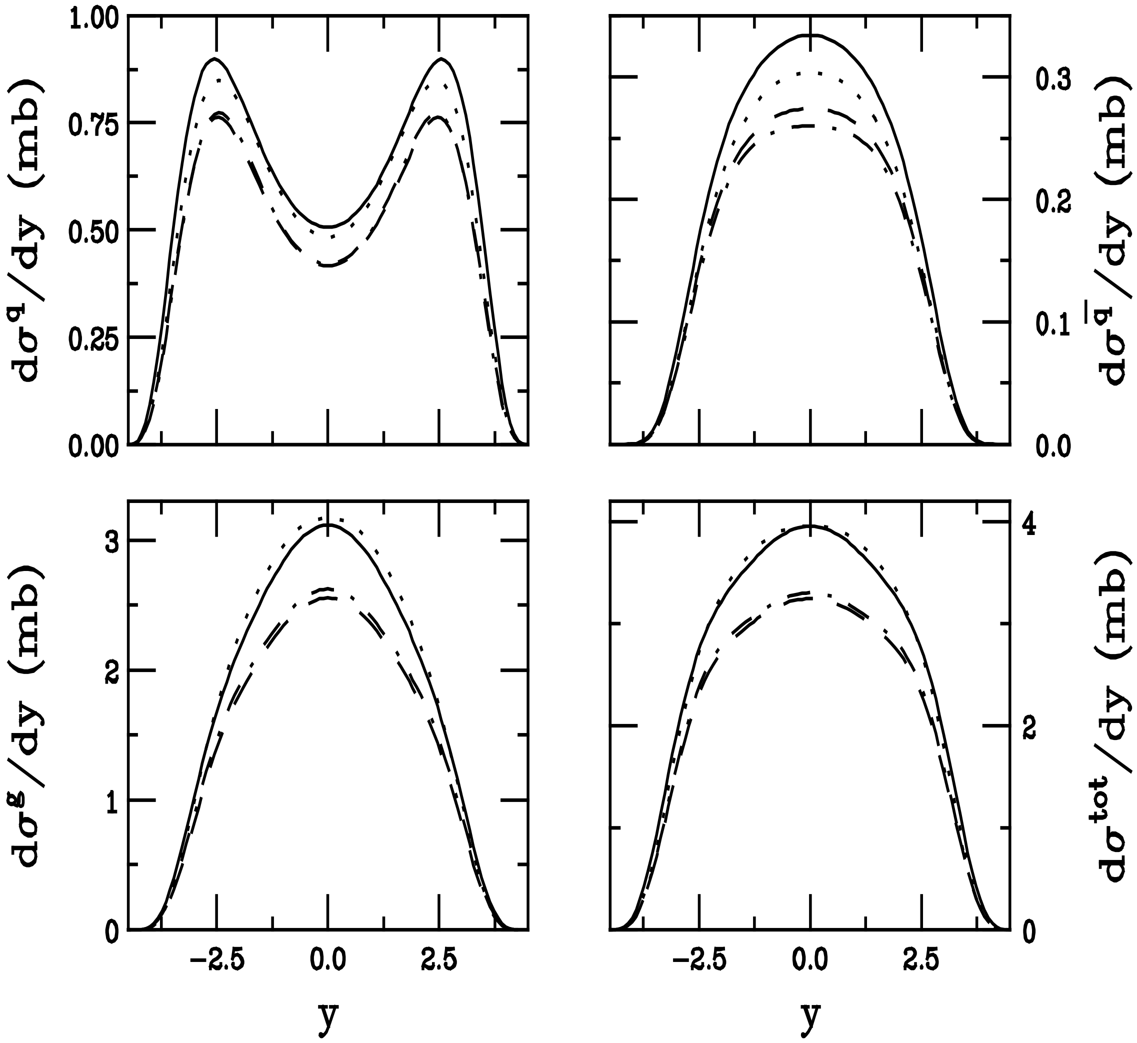

Figure 3: The rapidity distributions of quarks, antiquarks, gluons and the sum of all contributions in Au+Au collisions at $\sqrt{s_{NN}} = 200$ GeV integrated over b and divided by AB calculated with the MRST LO parton distributions for $p_0 = 2$ GeV. The solid curve is without shadowing, the dashed is with shadowing parameterization S_1, the dot-dashed is with S_2 and the dotted uses S_3.

Fragmentation

Produced partons have to become final-state hadrons

We convert the rapidity distribution to p_T and include fragmentation functions

$$\frac{d\sigma^h_{AB}}{dp_T} = 2p_T \int_0^\pi \frac{d\theta_{\rm cm}}{\sin\theta_{\rm cm}} \int dx_a \int dx_b f_{a/A}(x_a,Q^2) f_{b/B}(x_b,Q^2) \frac{D_{h/c}(z_c)}{z_c} \frac{d\hat{\sigma}}{d\hat{t}}$$

Integral over center-of-mass scattering angle $0 \leq \theta_{\rm cm} \leq \pi$ corresponds to integral over all rapidities. For $|y| \leq 1$, $\pi/4 \leq \theta_{\rm cm} \leq 3\pi/4$.

Parton densities, $f_{a/A}(x,Q^2)$, in a nucleus are $f_{a/A}(x_a) = S^a(x_a)(Z_A f_{a/p}(x_a) + N_A f_{a/n}(x_a))/A$ where Z_A and N_A are the proton and neutron numbers in nucleus A, S^a is shadowing function.

Fragmentation functions, $D_{h/c}(z_c)$, are the probability for the production of hadron h from parton c. They are taken from e^+e^- data so that

$$\begin{array}{rcll}
\pi & \equiv & \frac{1}{2}[\pi^+(u\overline{d}) + \pi^-(\overline{u}d)] & \qquad D_{\pi/u} = D_{\pi/d} \\
K & \equiv & \frac{1}{2}[K^+(u\overline{s}) + K^-(\overline{u}s)] & \qquad D_{K/u} = D_{K/s} \\
p & \equiv & \frac{1}{2}[p(uud) + \overline{p}(\overline{u}\overline{u}\overline{d})] & \qquad D_{p/u} = 2D_{p/d}
\end{array}$$

Fractional Contributions to Charged Hadron Production

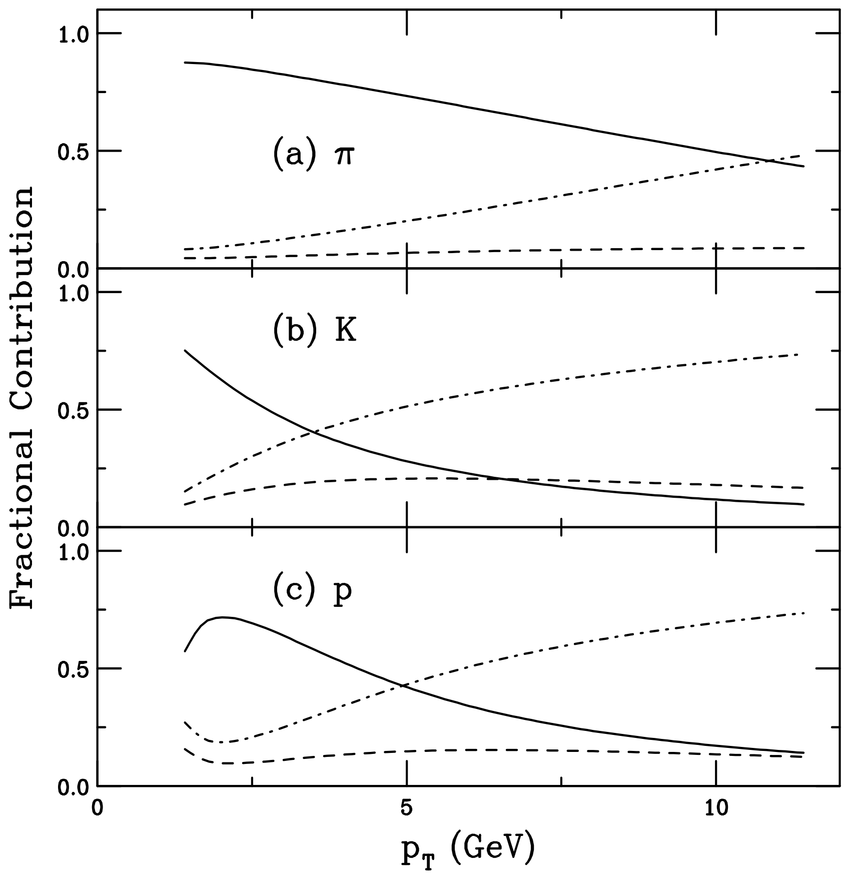

Figure 4: Fractional contribution of gluons (solid curves), quarks (dot-dashed curves) and antiquarks (dashed curves) for (a) charged pion, (b) charged kaon, and (c) proton production in pp collisions at $\sqrt{S} = 200$ GeV as a function of p_T.

Ratio Integrated Over all Rapidity

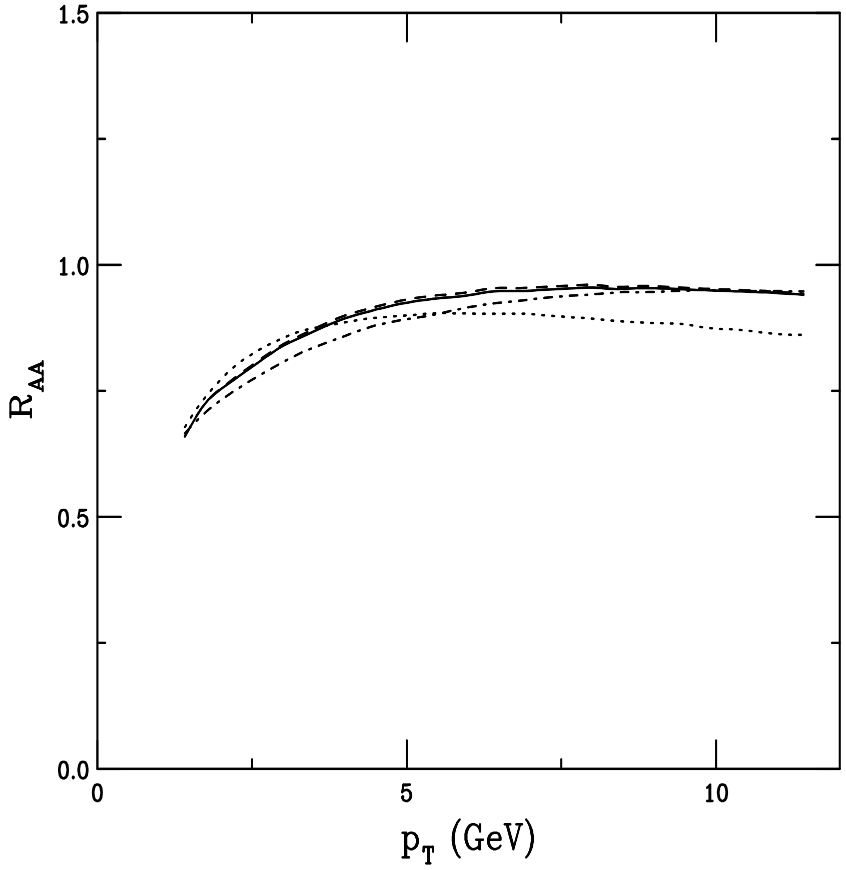

Figure 5: R_{AA} for pions (dashed curve), kaons (dot-dashed curve), protons (dotted curve) and the average over all hadrons (solid line) for gold-gold collisions at $\sqrt{S_{NN}} = 200$ GeV as a function of p_T. Spatially averaged shadowing is used.

Rapidity-Integrated Ratio for Shadowing Only

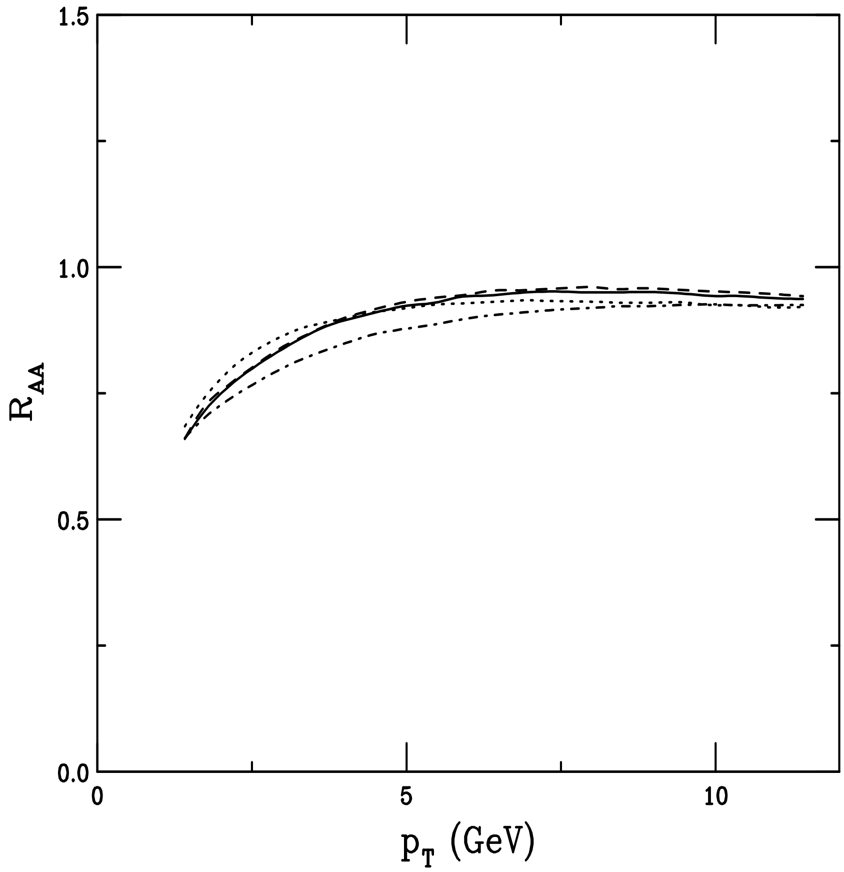

Figure 6: R_{AA} for pions (dashed curve), kaons (dot-dashed curve), protons (dotted curve) and the average over all hadrons (solid line) for gold-gold collisions at $\sqrt{S_{NN}} = 200$ GeV as a function of p_T. Spatially averaged shadowing is used. The gold-gold collision is treated as though $A = Z$.

Rapidity-Integrated Ratio for Isospin Only

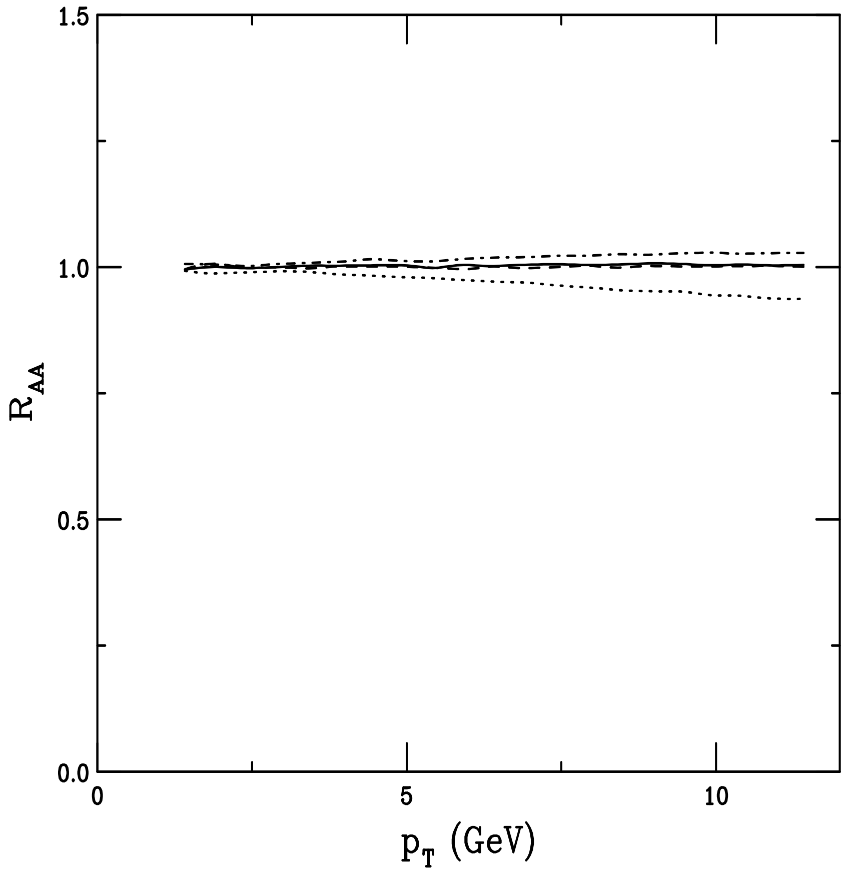

Figure 7: R_{AA} for pions (dashed curve), kaons (dot-dashed curve), protons (dotted curve) and the average over all hadrons (solid line) for gold-gold collisions at $\sqrt{S_{NN}} = 200$ GeV as a function of p_T. No shadowing is used.

Ratio Integrated Over $|y| \leq 1$

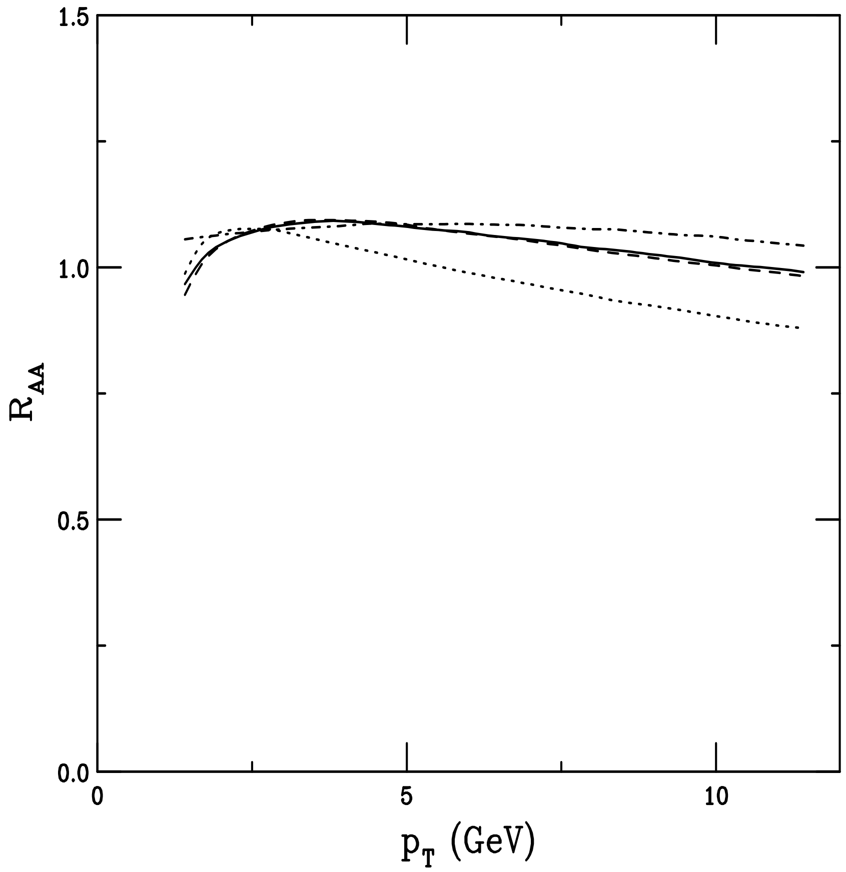

Figure 8: R_{AA} for pions (dashed curve), kaons (dot-dashed curve), protons (dotted curve) and the average over all hadrons (solid line) for gold-gold collisions at $\sqrt{S_{NN}} = 200$ GeV as a function of p_T in the interval $|y| \leq 1$. Spatially averaged shadowing is used.

Central Rapidity Interval for Shadowing Only

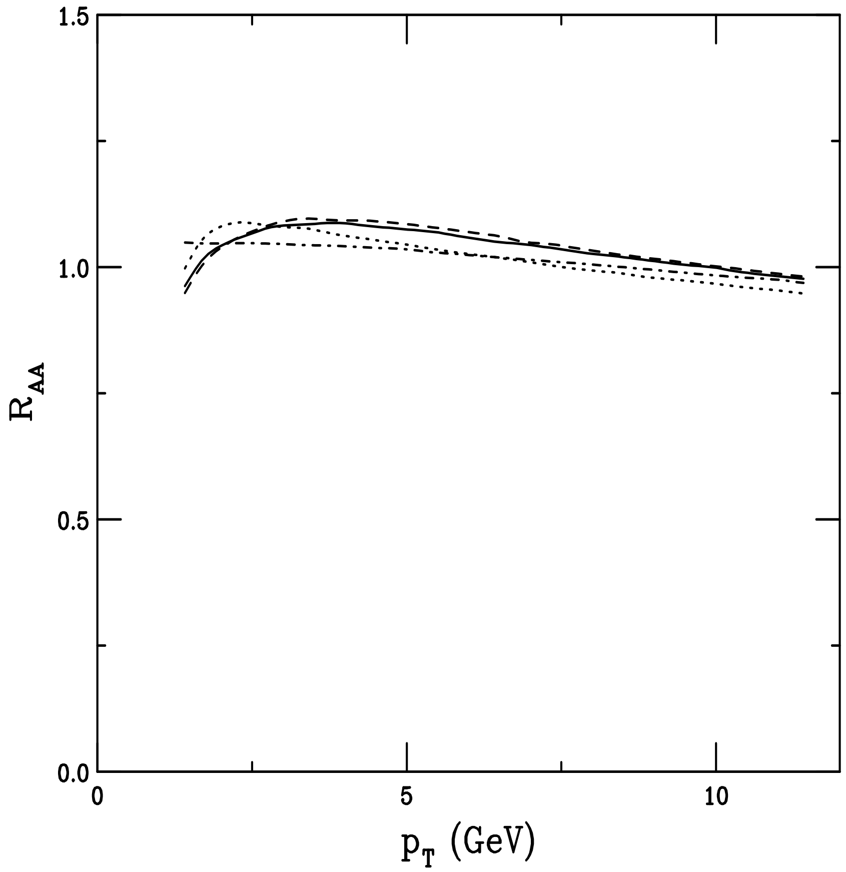

Figure 9: R_{AA} for pions (dashed curve), kaons (dot-dashed curve), protons (dotted curve) and the average over all hadrons (solid line) for gold-gold collisions at $\sqrt{S_{NN}} = 200$ GeV as a function of p_T in the interval $|y| \leq 1$. Spatially averaged shadowing is used. The gold-gold collision is treated as though $A = Z$.

Central Rapidity Interval for Isospin Only

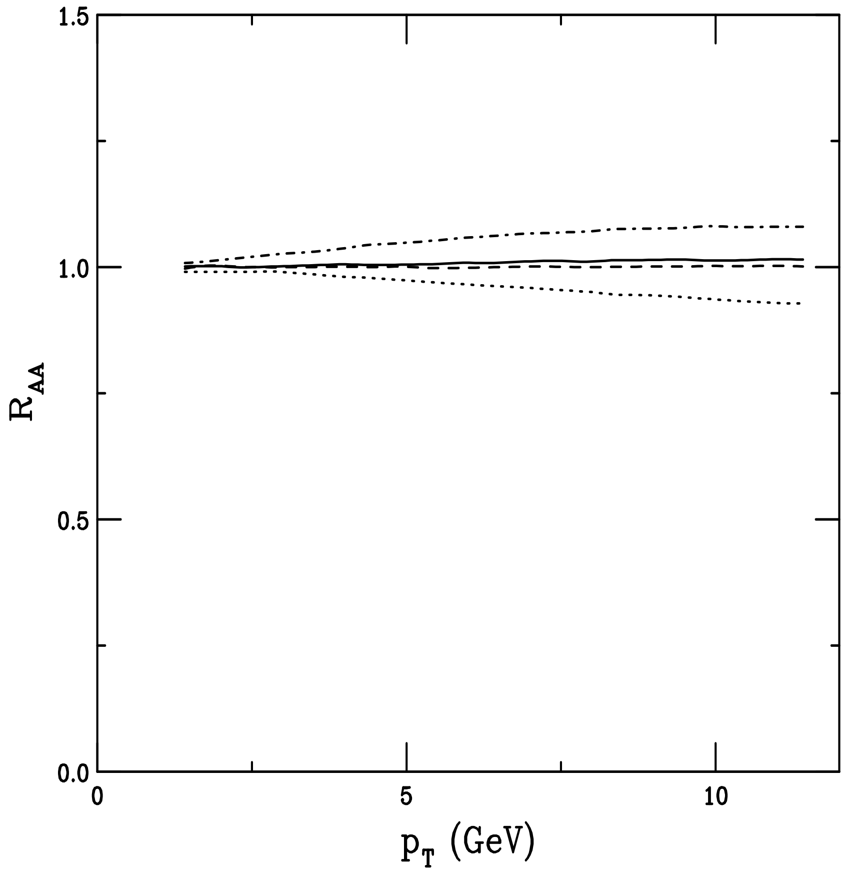

Figure 10: R_{AA} for pions (dashed curve), kaons (dot-dashed curve), protons (dotted curve) and the average over all hadrons (solid line) for gold-gold collisions at $\sqrt{S_{NN}} = 200$ GeV as a function of p_T in the interval $|y| \leq 1$. No shadowing is used.

Summary

- Calculated R_{AA} depends on the rapidity interval
- Shadowing is stronger effect when all rapidities included
- Isospin stronger effect in the interval $|y| \leq 1$
- Neither effect is strong enough to explain strong suppression at high p_T